SAND95-2181C
CONF-9508133--6

1995 COAL LIQUEFACTION AND GAS CONVERSION CONTRACTORS REVIEW CONFERENCE

Title: Synthesis and Characterization of Fe Colloid Catalysts in Inverse Micelle Solutions

Authors: Anthony Martino, Matthew Stoker, Michael Hicks, Calvin H. Bartholomew, Allen G. Sault, Jeffrey S. Kawola

Organization: Sandia National Laboratories, Albuquerque, NM 87185-0710

Contract No.: DE-AC04-76DP00789

Period of Performance: 10/1/90 - Present

RECEIVED
OCT 11 1995
OSTI

Objective:

Surfactant molecules, possessing a hydrophilic head group and a hydrophobic tail group, aggregate in various solvents to form structured solutions (1-3). In two component mixtures of surfactant and organic solvents (e.g., toluene and alkanes), surfactants aggregate to form inverse micelles. Here, the hydrophilic head groups shield themselves by forming a polar core, and the hydrophobic tails groups are free to move about in the surrounding oleic phase. We have studied the formation of Fe clusters in inverse micelles. Iron salts are solubilized within the polar interior of inverse micelles, and the addition of the reducing agent $LiBH_4$ initiates a chemical reduction to produce monodisperse, nanometer sized Fe based particles. The reaction sequence is sustained by material exchange between inverse micelles. The surfactant interface provides a spatial constraint on the reaction volume, and reactions carried out in these micro-heterogeneous solutions produce colloidal sized particles (10-100Å) stabilized in solution against flocculation by surfactant. We have characterized the clusters with respect to size with transmission electron microscopy (TEM) and with respect to chemical composition with Mossbauer spectroscopy, electron diffraction, and x-ray photoelectron spectroscopy (XPS). In addition, we have tested these iron based clusters for catalytic activity in a model hydrogenolysis reaction. The hydrogenolysis of naphthyl bibenzyl methane is used as a model for coal pyrolysis.

Metal alkoxide reactions (4), the formation of polymer particles (5,6), and the formation of metal (7-12) and semiconductor (13-21) clusters are examples of chemical processes that have been carried out in structured surfactant solutions. The formation of ultra-small metal particles is of particular interest in the area of chemical catalysis. The clusters are high surface area, highly dispersed, unsupported materials. In addition, catalytic enhancement due to unique material properties (i.e. quantum size effects) is possible. Metal clusters prepared by a number of techniques have been studied as potential

DISTRIBUTION OF THIS DOCUMENT IS UNLIMITED JK

MASTER

DISCLAIMER

This report was prepared as an account of work sponsored by an agency of the United States Government. Neither the United States Government nor any agency thereof, nor any of their employees, makes any warranty, express or implied, or assumes any legal liability or responsibility for the accuracy, completeness, or usefulness of any information, apparatus, product, or process disclosed, or represents that its use would not infringe privately owned rights. Reference herein to any specific commercial product, process, or service by trade name, trademark, manufacturer, or otherwise does not necessarily constitute or imply its endorsement, recommendation, or favoring by the United States Government or any agency thereof. The views and opinions of authors expressed herein do not necessarily state or reflect those of the United States Government or any agency thereof.

DISCLAIMER

Portions of this document may be illegible in electronic image products. Images are produced from the best available original document.

catalysts (22). Reactant adsorption and the reactivity in various processes depends strongly on particle size. The effect is not just a matter of surface area, but of a fundamental change in the material's properties as the number of metal atoms per cluster decreases. Pt, Pd, Rh, and Ir particles prepared via inverse micelle techniques (23) have been studied in the hydrogenation and isomerization of but-1-ene (24,25) and the hydrogenolysis and isomerization of hexanes (26). The activity of these catalysts increases when supported, and the selectivity of the colloidal sized particles is a function of the particle size. We are studying iron clusters as potential catalysts in hydrogenation reactions, Fischer-Tropsch synthesis, and coal liquefaction.

Experimental:

Octane and toluene were purchased from Aldrich at 99.9+% purity. Surfactants used include didodecyldimethylammonium bromide (DDAB) from Kodak and butyl-ethylene glycol n-dodecyl ether ($C_{12}E_4$) from Nikkol. Metal salts used include iron(III) chloride hexahydrate from Aldrich and iron(II) tetrafluoroborate hexahydrate from Alfa Chemicals. Lithium borohydride in tetrahydrofuran (2M) was purchased from Aldrich.

Synthesis of Fe Based Colloids: Four different iron samples (FeI, FeII, FeIII, and FeIV) were prepared and studied (Table 1). The reactions and all chemical manipulations are carried out in a glove box under dry, oxygen-free conditions. The synthesis technique is general and specific samples differ only in the type and concentration of salts and surfactant added to the apolar solvents. First, the inverse micelle solutions are prepared by adding surfactant to the solvents (i.e. DDAB in toluene, $C_{12}E_4$ in octane). Then, the metal salts are introduced and the precursor salt solutions are mixed overnight on a stirring plate to assure complete solubilization. Transparent yellow Fe salt solutions are formed. 2M $LiBH_4$/THF solution is directly injected into the salt solutions under rapid stirring to initiate the reduction of iron. The reaction is run at a 3:1 molar ratio of $[BH_4^-]$:$[Fe^+]$. The reacted Fe solutions turn black. The colloids formed in solution are stabilized by surfactant indefinitely.

Further manipulation of the iron in DDAB/toluene solutions produces iron powders. When approximately 15 vol. % methanol is added to the colloidal solution, the surfactant is washed from the colloid surface, and the particles aggregate. A black precipitate forms below a clear and transparent solution after several hours. The precipitate is separated from the solution by centrifugation and washed with methanol. The process is repeated two or three times, and the powder is finally dried (FeIII). We have re-coated the particles with poly(vinylpyrrolidone) (MW = 40,000) by adding the polymer to an iron powder and methanol mixture. The particles remain in solution for days without the

presence of surfactant. Removing the methanol produces Fe particles embedded in PVP powder (FeIV). Replacing surfactant with polymer allows us to control the ratio of stabilizing agent to metal, remove the relatively volatile surfactant for x-ray photoelectron spectroscopy studies, and protect the particles from oxidation during air exposure.

Table 1. Listing of the samples used in this study.

NAME	DESCRIPTION
FeI	0.01M $FeCl_3$, 10 wt. % DDAB/toluene
FeII	0.01M $Fe(BF_4)_2$, 10 wt. % $C_{12}E_4$/octane
FeIII	FeI powder from methanol washing
FeIV	0.03M $FeCl_3$, 10 wt. % DDAB/toluene, re-dispersed with PVP and re-dried

Characterization of the Colloids: Particle size and composition in the colloidal solutions are characterized with transmission electron microscopy (TEM) and electron diffraction. These tests are performed with a Joel 1200EX electron microscope. The colloidal solutions are applied directly on a holy carbon grid, and the solution is wicked away by adsorbent towels under the grid leaving the particles on the grid. Transfer of the particle coated grid into the microscope briefly exposes the sample to air.

Mossbauer spectroscopy is used to determine the composition of the iron in the PVP coated iron powders (FeIV). The Mossbauer Spectrometer (Austin Science) and its operation are described in detail elsewhere (27). The spectra are obtained using a 60 mCi ^{57}Co in palladium foil source and computer fitted to Lorentzian lines with a least-squares optimization procedure. The spectra are corrected during the collection procedure to remove the curved background of instrumental origin, and resonant absorption areas are found from integration of the background curvature-corrected spectra. With the use of an absolute laser velocity calibrator it is possible to measure isomer shifts to within an absolute accuracy of +/-0.005 mm/s. A particle embedded polymer powder was tested under four conditions: at room temperature without air exposure, at room temperature after air exposure, at -183°C, and at -183°C with an applied magnetic field of 11kGauss.

X-ray photoelectron spectroscopy (XPS) is used to determine the composition of the iron particles in solution (FeI), as powders (FeIII), and as powders re-dispersed with PVP in methanol (FeIV). To prepare samples of the surfactant stabilized iron particles suitable for XPS analysis, the surfactant/particle solution is evaporated to concentrate the particles and a drop of the resulting solution is placed on a Ta foil and allowed to evaporate

completely overnight. For analysis of the washed iron powders, the particles are re-dispersed in methanol and a drop of the dispersed solution is placed on a Ta foil and again allowed to dry. Finally, for the particles embedded in PVP, the PVP matrix is dissolved in methanol and a drop of the resulting solution placed on a Ta foil and the methanol evaporated to form a PVP film. All samples are prepared and mounted on a sample holder inside a dry, oxygen free glove box. As with microscopy, transfer of the sample to the XPS chamber requires brief exposure to air. XPS is performed using Al K_α radiation, and an analyzer resolution of 1 eV.

Complexometric experiments were used to determine the extent of reaction of the iron salts upon reduction. 1, 10 phenanthroline forms a complex with ionic Fe^{2+} species that has a distinctive maximum at 530 nm. The peak is followed before and after reaction with UV-visible spectrophotometry (Hewlett-Packard 8452A diode array spectrophotometer) by adding 1, 10 phenanthroline to the Fe salt precursor solutions and reacted Fe colloid solutions. The quantity and nature of the Fe^{2+} species present is determined. Two salt solutions were studied: $FeCl_3$ and $Fe(BF_4)_2$ in 10 wt. % $C_{12}E_4$ / octane.

Finally, BET surface area analysis of the methanol washed iron powder was carried out with a Quantachrome Autosorb-6 surface analysis apparatus.

Naphthyl Bibenzyl Methane (NBM) Hydrogenolysis: Hydrogenolysis testing of NBM has been developed as a model reaction for coal liquefaction (28). We add 100 mg of NBM, 400 mg of the hydrogen donating solvent 9,10 dihydrophenanthrene (9, 10 DHP), and up to 15 wt. % catalyst on an NBM basis to a 10 ml flame sealed glass test tube. If used, 15 mg of elemental sulfur is added. The test tube is sealed under ambient air pressure. The tube is placed in a 400°C sand bath for one hour. Previously, NBM hydrogenolysis has been used to study the selectivity of catalysts for five different cleavage reactions (28). We do not quantify the selectivity of the catalysts used here. Conversion is calculated as the ratio of the molar sum of all products to the initial amount of NBM. The products are worked up in THF and analyzed by gas chromatography. Methanol washed Fe powders were tested as catalysts. These results were compared to the commercial catalyst Shell 324 (12.4 wt. % Mo, 2.8 wt. % Ni on Al_2O_3).

Accomplishments:

Transmission electron micrographs show that the product of the reaction is highly dispersed nanometer sized particles of uniform size and shape (Figure 1). The number average diameter by TEM is 1.5 +/- 0.2 nm (FeI). Fe particle size as determined by TEM shows no discernible trend and is roughly constant in the ranges of 0.001M - 0.01M $FeCl_3$

salt concentration and 1-10 wt. % DDAB in toluene. In this range, the average particle diameter is 2.4 nm. The methanol extracted Fe powder characterized by TEM and BET surface analysis consist of agglomerated particles (FeIII). Large agglomeration structures approximately 100 nm in size are observed. These structures consist of the ultra small particles (approximately 2 nm in diameter) flocculated together. Multi-point BET analysis gives a surface area of 156 m^2/gm for this sample. The degree of re-dispersion upon addition of PVP has not been determined. As the particles are stable in solution for only a couple of days with PVP, it is likely that the degree of dispersion is not as great as after the original reaction in the presence of surfactant.

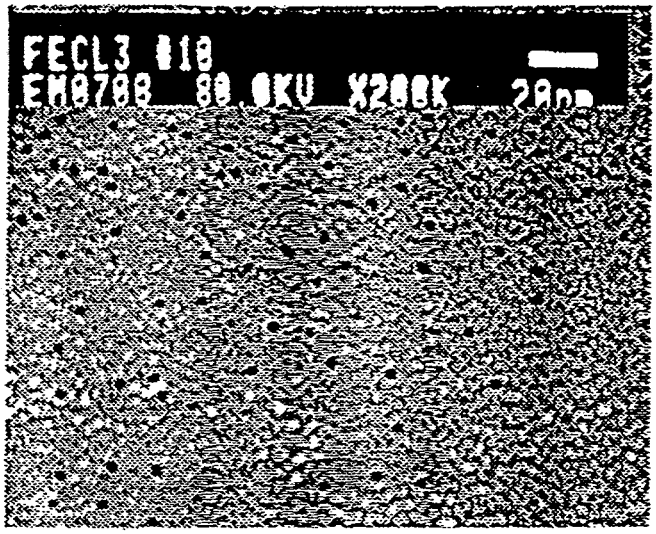

Figure 1. TEM of FeI particles. The number average diameter of the particles shown is 1.5 +/- 0.2 nm.

Mossbauer spectroscopy completed on the particle embedded polymer powder indicates the presence of three different forms of iron (FeIV). The spectrum for the powder at 21°C before exposure to air (Figure 2) is fit with two doublets and a singlet (corresponding Mossbauer parameters are found in Table 2). We assign the first doublet to the presence of fine superparamagnetic particles of FeB, the second doublet to the presence of Fe(II)BO_x, and the singlet to the presence of superparamagnetic Fe metal. On the basis of spectral areas, the iron phases are present at 60, 10, and 30 mole %, respectively with the species order listed above. The mole percentages are based on equal recoil-free fractions of each phase, and this assumption is only approximately correct in the case of small clusters. There is no discernible change in the spectra or fit after the sample is exposed to air. The iron is apparently protected from oxidation by the polymer. The spectrum of the sample at -183°C after exposure to air is quite different from the room temperature spectrum (Figure 3). It appears that the two large peaks in the room

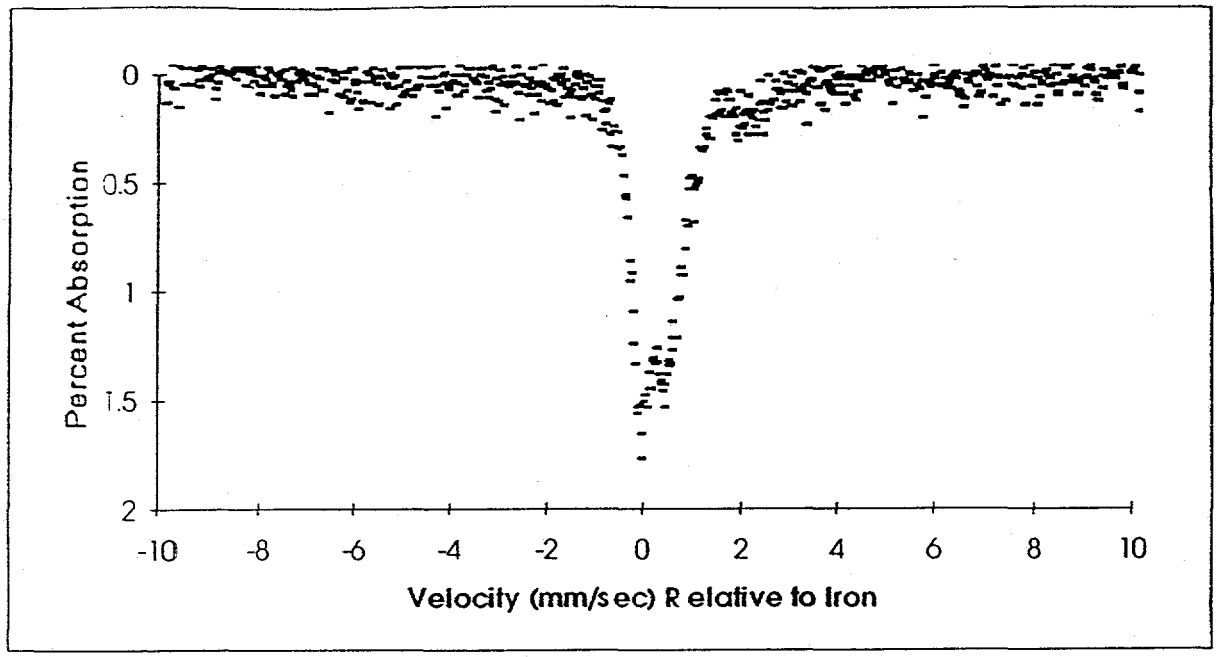

Figure 2. Mossbauer Spectrum of FeIV. T = 21°C. Not exposed to air. Parameters listed in Table 2.

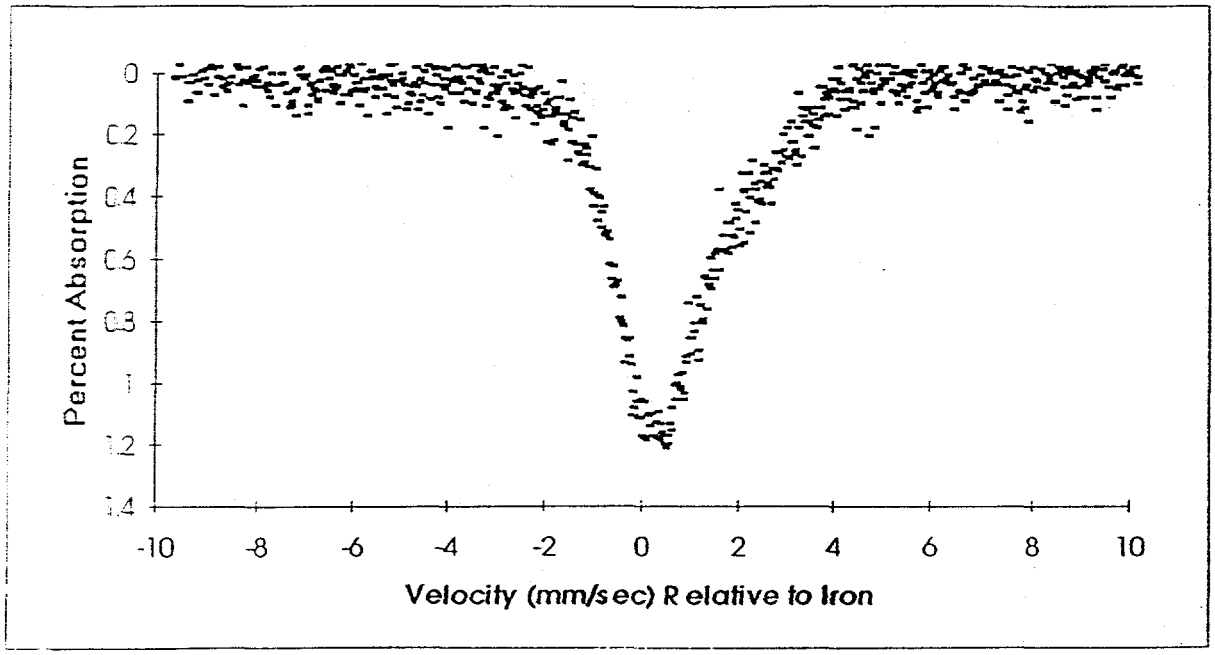

Figure 3. Mossbauer Spectrum of FeIV. T = -183°C. Exposed to air. Parameters listed in Table 3.

temperature spectrum have broadened. The broadened spectrum is fit with a sextet and two doublets (Table 3). The sextet has a magnetic hyperfine splitting of 128 kOe and an isomer shift of 0.35 mm/sec consistent with the presence of superparamagnetic FeB. When a magnetic field is applied to the sample, the spectrum is further broadened.

Table 2. Mossbauer Parameters for FeIV (Figure 2). T = 21°C, sample not exposed to air.

Assignment	Isomer Shift[a] (mm/sec)	Quadrupole Splitting (mm/sec)	Magnetic Hyperfine Splitting (kOe)	% Area
Doublet 1	0.450	0.27	----	60.4
Doublet 2	1.108	2.11	----	10.4
Singlet	-0.136	----	----	29.2

[a]relative to iron

Table 3. Mossbauer Parameters for FeIV (Figure 3). T = -183°C, sample exposed to air.

Assignment	Isomer Shift[a] (mm/sec)	Quadrupole Splitting (mm/sec)	Magnetic Hyperfine Splitting (kOe)	% Area
Sextet	0.98	0.065	94.0	43.5
Doublet	0.29	0.87	----	56.5

[a]relative to iron

Selected area electron diffraction (FeII) and XPS (FeI, FeII, FeIV) give complementary results. Diffraction patterns of particles deposited on the microscope grid are consistent with the presence of α-Fe. The electron diffraction results do not indicate the presence of any crystalline iron oxides, borides, or borates. A diffraction pattern consistent with the presence of crystalline B_2O_3 as a reaction by-product is also detected. XPS of *in-situ* colloids in solution, methanol washed powders, and particle embedded polymer powders detects an undetermined Fe^{2+} species only.

Complexometric experiments indicate that the reaction is complete upon the addition of $LiBH_4$. In the $Fe(BF_4)_2$ precursor solutions, the Fe^{2+} species complexes with 1,10 phenanthroline, and the distinctive peak is observed at 530 nm. The peak is non existent in $Fe(BF_4)_2$ samples after the addition of $LiBH_4$ indicating the reaction goes to completion. In $FeCl_3$ precursor solutions, no complex is formed with the Fe^{3+} species. After reaction, a slight peak at 530 nm is detected indicating some conversion of Fe^{3+} to Fe^{2+} but too little to quantify.

Hydrogenolysis of naphthyl bibenzyl methane (NBM) was tested with the methanol extracted Fe powder (FeIII) with and without sulfur additives and compared with the commercial catalyst Shell 324. In each experiment we monitored the percentage recovery of the reactant NBM and the percentage conversion to products (28) by gas chromatography. In each experiment we also monitored the percentage recovery of the hydrogen donating solvent 9, 10 DHP and the percentage converted to its dehydrogenated form phenanthrene. In an average of six runs, NBM was recovered at nearly 97+/-3% in thermal runs (no catalyst) and no product was obtained (Figure 4). Some NBM was converted to products in thermal runs with added elemental sulfur. Little 9, 10 DHP is dehydrogenated to phenanthrene in the thermal runs. Methanol extracted Fe powder as catalyst decreased the amount of NBM recovered to 87% and to 75% with added S. Product recovery correspondingly increased. In the Fe sample tests, hydrogens are given up to the hydrogenolysis products, and some 9, 10 DHP is dehydrogenated to phenanthrene.

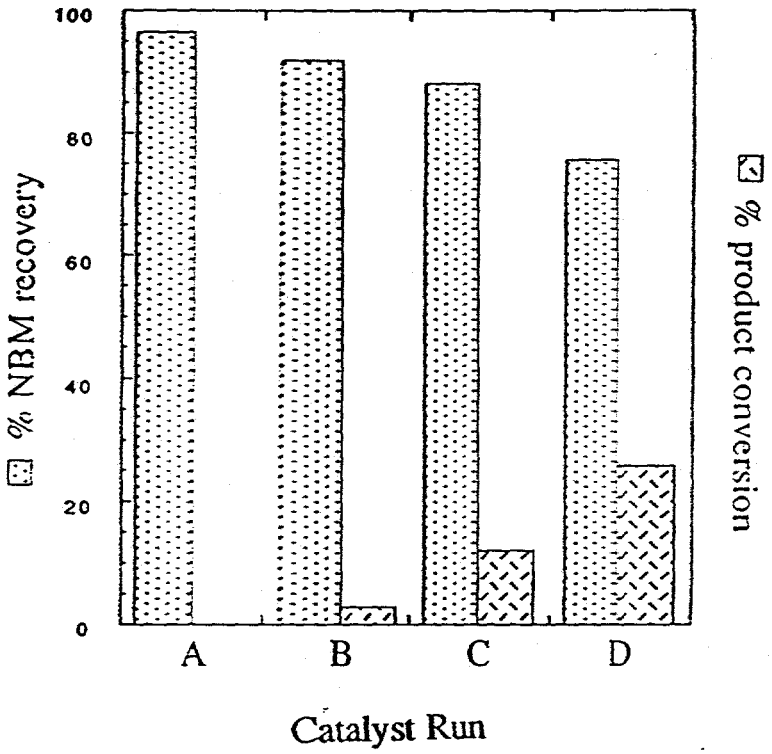

Figure 4. NBM hydrogenolysis results for Fe clusters. (a) The percentage of reactant recovered and percentage converted to product. A = thermal average; B = thermal with elemental S average; C = FeIII (~ 15% active metal basis); D = FeIII with elemental S (~ 15% active metal basis).

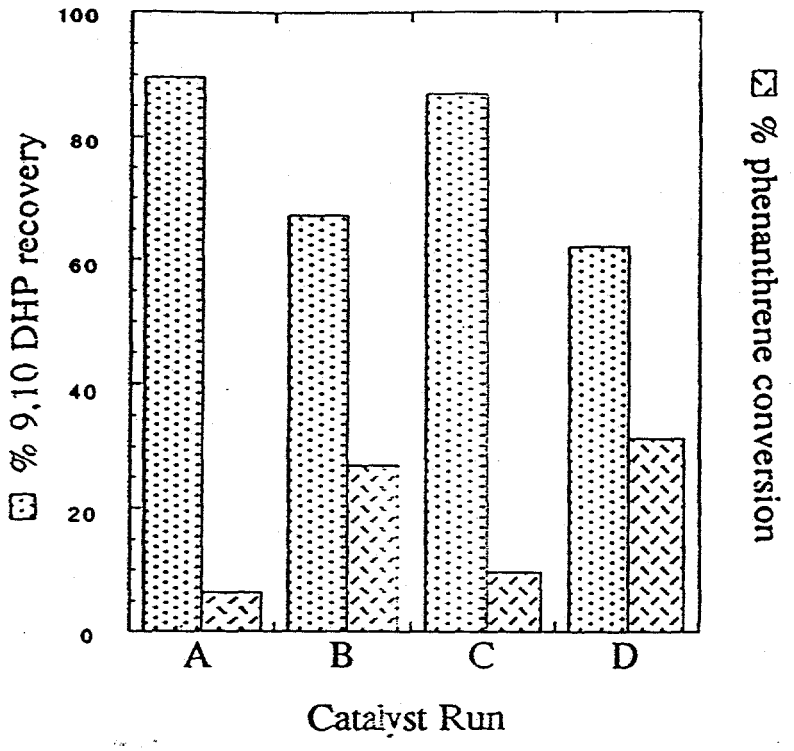

Figure 4. NBM hydrogenolysis results for Fe clusters. (b) The percentage of the hydrogen donating solvent 9, 10 DHP recovered and the percentage dehydrogenated to phenanthrene. A = thermal average; B = thermal with elemental S average; C = FeIII (~ 15% active metal basis); D = FeIII with elemental S (~ 15% active metal basis).

Much higher product yields were obtained with Shell 324 (Figure 5). Higher conversions of 9,10 DHP to phenanthrene are consistent with these higher yields. In order to study the effect of surfactant on catalytic activity, we doped Shell 324 with increasing amounts of DDAB. As the Shell 324:DDAB mass ratio decreases, the trends in reactant recovery and product conversion move back to the thermal results indicating loss of catalytic activity. Initially the conversion of 9, 10 DHP to phenanthrene moves toward the thermal results as well. At the lower Shell 324 : DDAB ratios, however, this trend reverses itself and nearly all of the 9,10 DHP is converted to phenanthrene.

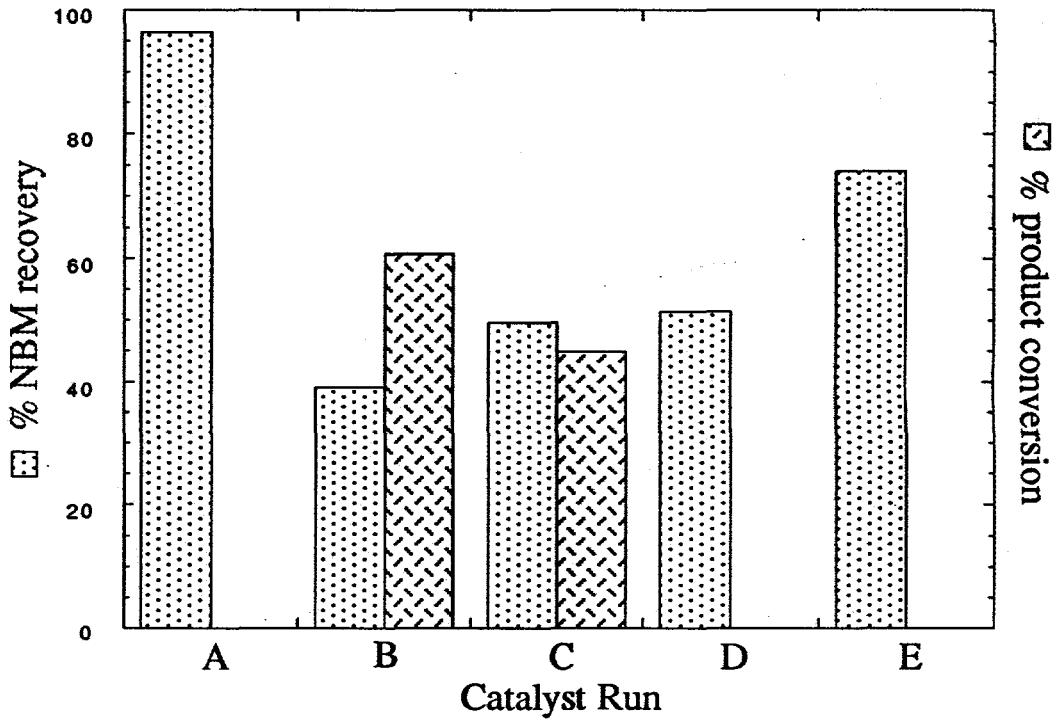

Figure 5. NBM hydrogenolysis results for Shell 324 as a function of DDAB surfactant doping. (a) The percentage of reactant recovered and percentage converted to product. A = thermal average; B = Shell 324; C = Shell 324:DDAB =1:4; D = Shell 324:DDAB = 1:20; E = Shell 324:DDAB = 1:50. Active metal basis ~ 15% for all catalyst runs.

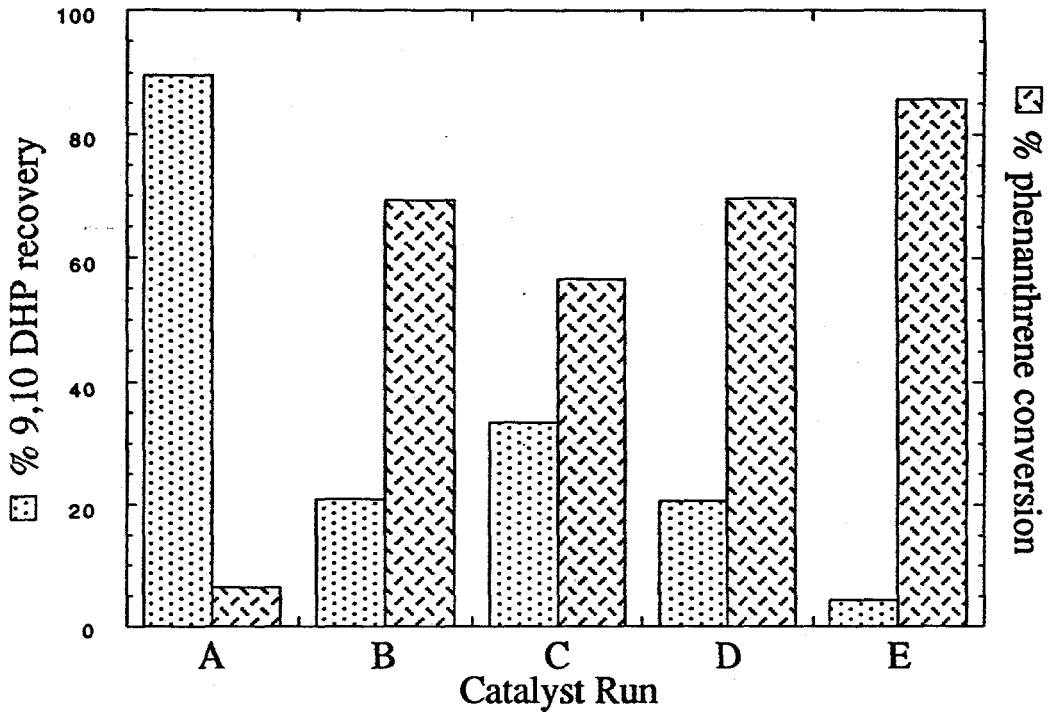

Figure 5. NBM hydrogenolysis results for Shell 324 as a function of DDAB surfactant doping. (b) The percentage of the hydrogen donating solvent 9, 10 DHP recovered and the percentage reduced to phenanthrene. A = thermal average; B = Shell 324; C = Shell 324:DDAB =1:4; D = Shell 324:DDAB = 1:20; E = Shell 324:DDAB = 1:50. Active metal basis ~ 15% for all catalyst runs.

Conclusions:

Introduction of $LiBH_4$ to iron salt containing inverse micelle solutions causes immediate reduction of the salt to form nanometer sized, highly dispersed particles of equal size and shape. $LiBH_4$ enters the surfactant-oil solution and is solubilized within the inverse micelle structure. The reaction is initiated and is sustained through material exchange between inverse micelles. After the particle growth has equilibrated, the surfactant stabilizes the particles and prevents flocculation and precipitation. The final particle size of nanometer sized clusters formed in inverse micelles depends on a complicated nucleation and growth process (29). Inverse micelles effect this process primarily in two ways: (1) diffusion of the reacting nucleation sites and ions is governed by exchange rates between micelles and (2) the critical nucleation size depends inherently on the size of the inverse micelles. Size dependence of metal borides, CdS, and CdSe clusters

produced in inverse micelles has been discussed previously (12-21). The Fe particles synthesized in DDAB/toluene mixtures showed no size dependence by TEM on the salt to surfactant concentration ratio within the range studied.

Mossbauer spectroscopy, electron diffraction, and XPS results indicate three products are formed by the reduction of iron salts with $LiBH_4$ in inverse micelle solutions. Mossbauer spectroscopy detects three phases: FeB, $Fe(II)BO_x$, and metallic Fe in approximate mole percentages of 60%, 10%, and 30%, respectively. Mossbauer results at low temperatures and in the presence of a magnetic field further support the presence of FeB. The spectral broadening is consistent with longer magnetic relaxation times in a superparamagnetic species, and the sextet has a hyperfine field consistent with FeB. In the limit of a sufficiently large magnetic field or at sufficiently low temperatures, the spectrum would resolve into six lines.

Electron diffraction gives strong evidence for the presence of α-Fe, and is consistent with the Mossbauer results showing the presence of metallic Fe. The FeB phase is not detected by diffraction because of relatively weak scattering. It is unlikely that the manipulation of the colloids in solution (tested in electron diffraction) to produce the particles in PVP (tested in Mossbauer) results in the formation of FeB and $Fe(II)BO_x$. Further Mossbauer experiments are planned, however, on particles not manipulated with methanol and PVP.

XPS of *in-situ* colloids in solution, methanol washed powders, and particle embedded polymer powders detects an undetermined Fe^{2+} species. XPS examines only the particles that protrude above the PVP surface as the Fe 2p photoelectrons can only escape from within 3-4 nm of the PVP film surface. The protruding particles are not protected from oxidation upon exposure to air, and the XPS detected phase is likely a mixture of oxidized FeB and α-Fe. The B 1s XPS spectrum confirms the presence of oxidized boron, but does not show any evidence for borides. Metallic iron detected by electron diffraction even though the samples are exposed to air is not detected by XPS. As XPS surveys only particle surfaces, perhaps an oxidized shell surrounds a small core of Fe^0 species (FeB and/or α-Fe).

Hydrogenolysis of NBM indicates catalytic activity with FeIII. A more than linear increase in activity with added S indicates that there is a synergistic effect between the Fe and S.

Catalyst activity of Shell 324 far exceeds the activity of the iron based clusters. Doping Shell 324 with surfactant illustrates the effect of surfactant on catalyst activity. When Shell 324 is doped with surfactant, catalyst activity decreases (Figure 5). The behavior of the hydrogen donating solvent indicates two mechanisms are at work. At low

surfactant concentrations, a decrease in product conversion and a decrease in the amount of 9, 10 DHP dehydrogenated to phenanthrene indicates less activity due to a chemical or steric poisoning of the catalyst. At high surfactant concentrations, we propose that a decrease in NBM conversion and an increase in the amount of 9, 10 DHP dehydrogenated to phenanthrene indicates that the thermal pyrolysis products of the surfactant (observed by GC) scavenge the hydrogens from the donor solvent.

References:

(1) Langevin, D., Accounts of Chemical Research, 21, 255 (1988)
(2) Fendler, J.H., Chem. Rev., 87, 877 (1987)
(3) Henglein, A., Chem. Rev., 89, 1861 (1989)
(4) Jean, J.H. and Ring, T.A., Colloids and Surfaces, 29, 273 (1988)
(5) Paleos, C.M., Chemical Society Reviews, 14, 45
(6) Perez-Luna, V.H., Puig, J.E., Castano, V.M., Rodriguez, B.E., Murthy, A.K., and Kaler, E.W., Langmuir, 6, 1040 (1990)
(7) Barnickel, P. and Wokaun, A., Molecular Physics, 69, 1 (1990)
(8) Gobe, M, Kon-No, K., Kandori, K. and Kitahara, A., Journal of Colloid and Interface Science, 93, 293 (1983)
(9) Kurihara, K., Kizling, J., Stenius, P., and Fendler, J.H., J. Am. Chem. Soc., 105, 2574 (1983)
(10) Nagy, J.B., Gourgue, A. and Derouane, F.G., Preparation of Catalysts III, eds. Grange, P., Jacobs, P.A., Elsevier Science Publishers,193 (1983)
(11) Torigoe, K. and Esumi, K., Langmuir, 8, 59 (1992)
(12) Nagy, J.B., Colloids and Surfaces, 35, 210 (1989)
(13) Lianos, P. and Thomas, J.K., Journal of Colloid and Interface Science, 117, 505 (1987)
(14) Lianos, P. and Thomas, J.K., Chemical Physics Letters, 125, 299 (1986)
(15) Modes, S. and Lianos, P., J. Phys. Chem., 93, 5854 (1989)
(16) Petit, C. and Pileni, M.P., J. Phys. Chem., 92, 2282 (1988)
(17) Petit, C., Lixon, P. and Pileni, M.P., J. Phys. Chem., 94, 1598 (1990)
(18) Motte, L., Petit, C., Boulanger, L., Lixon, P. and Pileni, M.P., Langmuir, 8, 1049 (1992)
(19) Pileni, M.P., Motte, L. and Petit, C., Chem. Mater., 4, 338 (1992)
(20) Robinson, B.H., Towey, T.F., Zourab, S., Visser, A.J.W.G. and van Hoek, A., Colloids and Surfaces, 61, 175 (1991)
(21) Towey, T.F., Khan-Lodhi, A. and Robinson, B.H., J. Chem. Soc. Faraday Trans., 86, 3757 (1990)
(22) Moskovits, M., Annu. Rev. Phys. Chem., 42, 465 (1991)
(23) Boutonnet, M., Kizling, J., Stenius, P. and Maire, G., Colloids and Surfaces, 5, 209 (1982)
(24) Boutonnet, M., Kizling, J., Touroude, R., Maire, G. and Stenius, P., Applied Catalysis, 20, 163 (1986)
(25) Boutonnet, M., Kizling, J., Mintsa-Eya, V., Choplin, A., Touroude, R., Maire, G. and Stenius, P., Journal of Catalysis, 103, 95 (1987)
(26) Boutonnet, M., Kizling, J., Touroude, R., Maire, G. and Stenius, P., Catalysis Letters, 9, 347 (1991)
(27) Neubauer, L.R., Ph. D. Dissertation, Brigham Young University, (1986)
(28) Faracasiu, M.; Smith, C. ACS Preprints Fuel Chemistry Division, 35, 404, (1990)
(29) Steigerwald, M.L. and Brus, L.E., Annu. Rev. Mater. Sci., 19, 471 (1989)